SUMMARY OF FINDINGS OF WAVE LOAD MEASUREMENTS ON THE TERN PLATFORM

Prepared by WS Atkins Consultants Ltd for the Health and Safety Executive

SUMMARY OF FINDINGS OF WAVE LOAD MEASUREMENTS ON THE TERN PLATFORM

Authors:

N.Atkins
R.A.Lyons
R.C.T.Rainey
WS Atkins Consultants Limited
Berkshire House
171 High Holborn
London WC1V 7AA

SUMMARY

A Joint Industry Project organised by Shell and WS Atkins has analysed the wave loads seen on Shell's Tern platform in the Northern North Sea, between February 1990 and April 1992. Over this period, there were 15 storms with significant waveheight above about 8m, and from each a worst-case 1-hour data record was taken. Within each of these 15 1-hour records, the 25 highest waves were selected - a total of 375 waves in all. Conventional Stokes design waves were then fitted to the height and period of each of these 375 waves, and the peak-to-peak wave load computed on the structure, using a full Morison finite-element model, and exactly following conventional UK design practice. This was compared with the measured peak-to-peak wave load (only oscillatory loads being available, because of the nature of the load sensors), both base shear force (BSF) and overturning moment (OTM), thus giving for each wave the ratio:

$$R_{cycle} = \frac{\text{measured load in single wave}}{\text{computed load in same wave}}$$

This parameter measures the wave load calculation conservatism in each individual wave cycle, and follows the standard practice of previous experiments. In addition, two parameters were devised to measure the conservatism in the extreme load seen over a whole 1-hour record. The simpler of these was:

$$R_{det} = \frac{\text{largest of the 25 measured loads in a 1-hour record}}{\text{largest of the 25 computed loads in a 1-hour record}}$$

Note that, unlike R_{cycle}, the measurement and computation *need not come from the same wave*. The other whole-record parameter was based on the largest wave in that record, as predicted by standard statistical methods, from the measured wave spectrum. The load in this theoretical wave was computed, to give:

$$R_{stat} = \frac{\text{largest of 25 measured loads in 1-hour record}}{\text{load computed in theoretical largest wave for that record}}$$

Thus the experiment yielded 375 values of R_{cycle}, and 15 each of R_{det} and R_{stat}. The mean and standard deviation of each of these 3 sets of results is shown in Table 1 below.

Table 1
Final conservatism parameters

Parameter	Mean value over experiment		Standard deviation over experiment		95% Confidence limits on mean value	
	BSF	OTM	BSF	OTM	BSF	OTM
R_{cycle}	0.77	0.80	0.20	0.23	±0.017	±0.020
R_{det}	0.96	1.01	0.11	0.17	±0.050	±0.077
R_{stat}	0.88	0.92	0.10	0.12	±0.045	±0.054

It may be seen that R_{det} and R_{stat} are noticeably higher, on average, than R_{cycle}. The difference is evidently significant statistically, because the Table also shows the 95% confidence limits on these mean values, which can be deduced from the standard deviations, given the number of results.

It should also be borne in mind that the "standard statistical methods" used to predict the theoretical highest wave in each record (and hence define R_{stat} , see above) were the simplest available, using the asymptotic Rayleigh formula. Conventional oceanographic practice is to reduce that simple Rayleigh prediction by a semi-empirical correction factor. If this procedure is followed here, the above values of R_{stat} will increase by about 10%, further emphasising the differences seen in the above Table.

It is important to recognise that the effect of current on the peak-to-peak wave loads considered in this experiment is small. This is because the current magnifies the load peaks of one sign, but almost equally reduces the load peaks of the other sign. The overall effect on the results in Table 1 is statistically insignificant, and the current was therefore taken as zero, for simplicity. The extreme load amplitude, on the other hand, which is of course the important parameter structurally, is much more strongly affected by the current. UK design practice is to take the current at its extreme value, even though it is unlikely to occur at the same time as the extreme wave. This leads to an important additional conservatism in UK practice, not seen in the above figures.

Finally, the Tern data has not been analysed to investigate the separate conservatisms in the Stokes wave kinematics calculation, and the Morison wave force calculation. However, in the largest and most-forceful wave seen during the experiment (26.92 m high, 12.50 s period), the measured water velocities correspond closely with a Stokes wave.

1. INTRODUCTION

The present approach to the design of fixed steel offshore structures is largely experience based, and there are indications that current design practice, as a whole, is conservative. It appears[1], for example, that some early Gulf of Mexico platforms have survived storms in which the significant wave height, at any rate (if not the maximum waveheight), was in excess of notional design values.

Shell accordingly undertook to instrument one of their newest platforms in the North Sea, the Tern steel jacket structure illustrated in Figure 1.1. The aim was to investigate one possible source of this conservatism, namely the wave loading calculation. The project was part of an international programme of research by the major oil companies, which was aimed at the extensive 1993 revision of the API Design Guidelines for fixed offshore platforms[2].

On behalf of Shell, WS Atkins (WSA) organised a Joint Industry Project to analyse the data collected from Tern, and use it to investigate the conservatism in conventional wave load calculations. The participants in the JIP were:

Shell UK Exploration and Production Ltd.[1]
Amoco (UK) Exploration Company
BP International Ltd
Conoco (UK) Ltd
The Health & Safety Executive
Elf UK plc
Texaco Britain Ltd
Chevron UK Ltd
British Gas plc
Amerada Hess Ltd
Mobil North Sea Ltd

The instrumentation contractor, responsible to Shell for data collection, was Fugro Structural Monitoring Ltd (SM). Preliminary data collation and analysis for the Joint Industry Project was also the responsibility of SM, under contract to WSA.

The WSA Final Report[3] on this work was delivered to Participants in May 1993. The present Report was prepared by WSA under contract to the Health and Safety Executive, to summarise this original Final Report, and its findings, for a wider audience.

[1] Operator in the UK sector of the North Sea for Shell and Esso

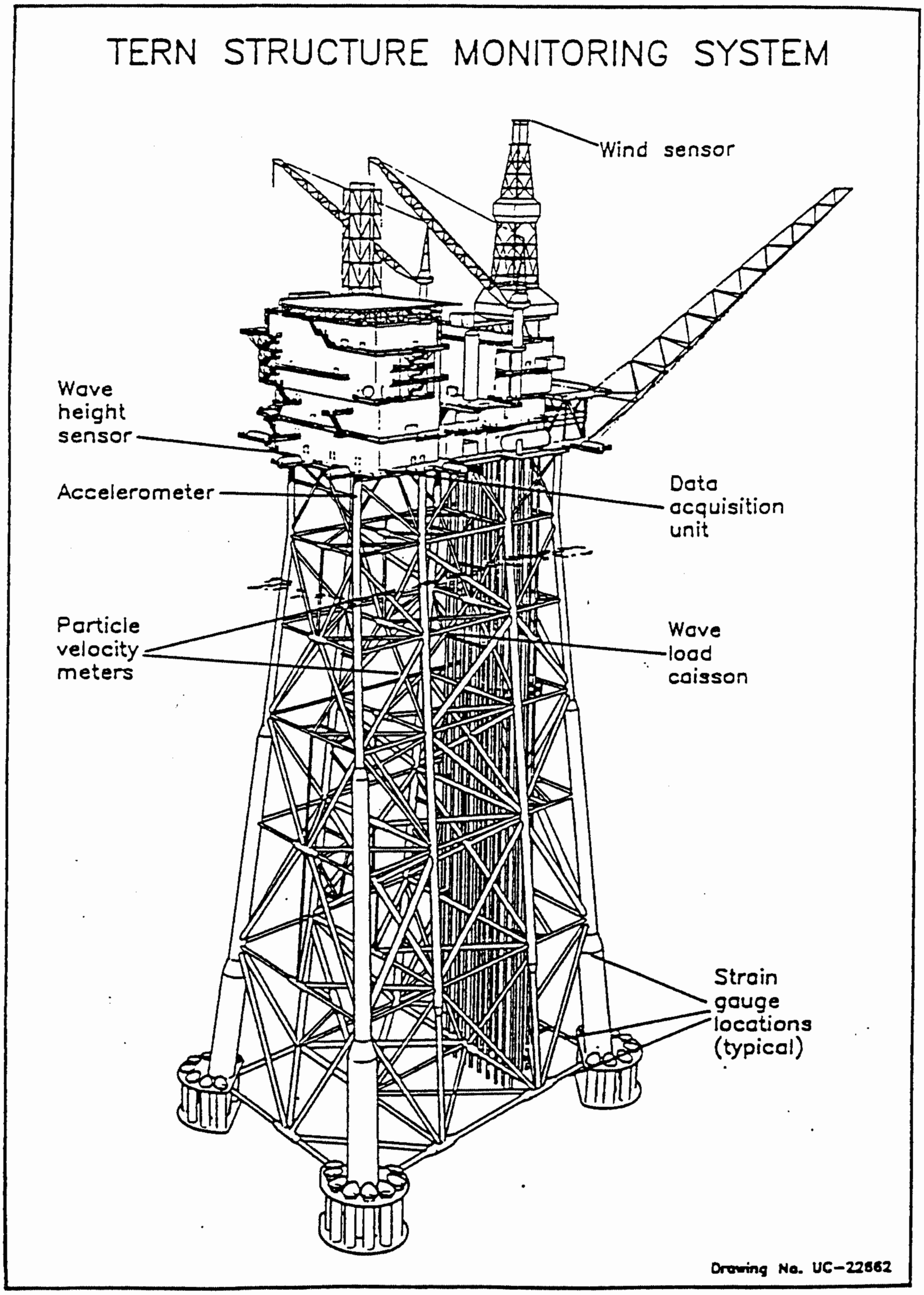

Figure 1.1
The Tern steel jacket structure
[Figure courtesy of Shell Expro]

2. DESCRIPTION OF TERN PLATFORM, INSTRUMENTATION AND DATA PROCESSING

Shell/Esso's Tern platform was installed in 1988 approximately 150km north-east of Shetland, in water of depth 167 m (at LAT). The steel, launch-installed sub-structure, weighing approximately 21,000 tonnes, supports a topside load of drilling and production facilities and accommodation for approximately 180 people.

The extreme design wave for the platform is consistent with a 50 year return period:

Wave Height	=	30.5m
Wave Period	=	17.7sec

2.1 MEASUREMENT SYSTEM

The Platform Measurement System comprises both environmental and structural sensors (see Figures 1.1 and 2.1) and a central data processing unit with a design life of 10 years. An important feature of the system is that the environmental sensors measure both steady and oscillatory components, whereas the structural sensors (because of the problem of strain gauge drift) measure oscillatory components only. Thus the investigation is primarily aimed at wave loads.

2.1.1 Environmental Sensors

A laser type wave height gauge manufactured by EMI was attached to the module support frame, in the location shown in Figure 2.1. This instrument gave a continuous record of water surface elevation.

Two water particle velocity meters (PVM) were located on specially-designed supports within the structure, in the locations shown in Figures 1.1 and 2.1, at depths of 13m and 41m below nominal LAT ("nominal LAT" is the platform datum, originally intended to correspond with the lowest astronomical tide level. The actual level of the lowest astronomical tide on the platform is a few centimetres below "nominal LAT").

As is generally the case with offshore environmental sensors, some problems were encountered, as follows:

- The EMI wave height gauge gave poor quality signals from time to time;
- The PVM's did not give meaningful static current values although the dynamic signals were of good quality;

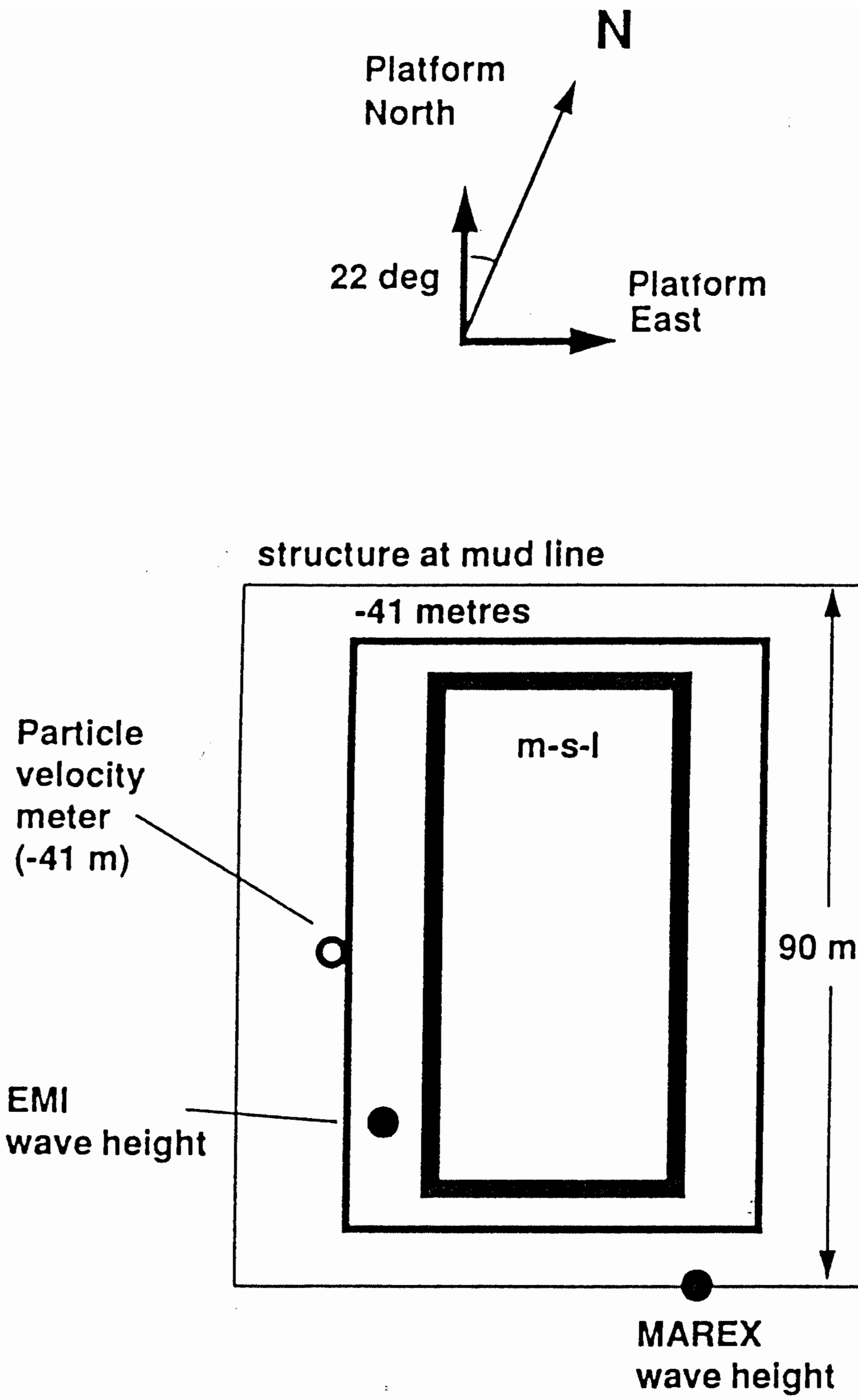

Figure 2.1
Layout of Sensors

Changes were accordingly made in 1991 to rectify the problems:

- In January the EMI wave sensor was replaced with a new one of the same type and an additional sensor of a different type was also installed. The additional sensor was a radar type manufactured by Marex and was installed on the module support frame near to the south-east corner of the platform, as shown in Figure 2.1. Although this instrument gave valuable additional data, it proved more sensitive to spray than the EMI sensor (see e.g. Figure 5.1 below), which accordingly remained the principal source of the results in this Report.

- In January the PVM's were replaced by some manufactured by Interocean. Unfortunately, however, the one at 13m depth failed in February.

After the changes were made, good quality data were obtained from both wave sensors and there was virtually continuous data collection throughout the 1991/92 winter period. One outstanding problem was the effect of spray on the signal of the windward wave sensor in high sea states which was overcome for the record 18th October 1991 by editing the wave data.

2.1.2 Structural Sensors

A total of 64 strain gauge rosettes were attached to structural members at the base of the four corner legs and lowest horizontal frame members. The strain gauge data was processed by SM to obtain the base shear force (BSF) and overturning moment (OTM) data for the global load assessment. The integrity of the processing algorithm used by SM was cross-checked by WSA, by means of a finite-element structural model of the platform, derived from the hydrodynamic model described in Section 3. Two nominal loads (representative of a wave load from the Southwest, with and without platform dead-weight) were applied to this finite-element model, and the strains found at the gauge positions. This data was then used as input to the SM algorithm, so as to give figures for the base shear and OTM, which could be compared with the base shear and OTM applied to the finite-element model. The agreement was within 6% for all components of these variables - e.g. 5.5% for base shear in platform north, and 1.4% for base shear in platform east. See WSA Final Reports(3), in particular Appendix F in 28/6/91 issue of Report G3356/RPT/005.

It has been noted in the literature(4) that no "pull test" was applied to the Tern platform, to check the strain gauges themselves, as well as the processing algorithms. However, different gauges are used on Tern to measure end-on and broadside wave loads, and the results obtained in the two cases can be compared statistically, to check for any signs of different gauge sensitivity. This is done in Appendix 1, where it is concluded that the sensitivity is the same. This suggests that the strain gauge system was functioning accurately on both headings.

2.1.3 Data Acquisition Unit

All data are collected in the Data Acquisition Unit (DAU) located at the lowest deck of the Tern topsides.

All measurements were processed on an hourly basis and these hourly statistical summaries were stored on magnetic tape, thus reducing the amount of data storage. However, if the waves exceeded a certain pre-set value, all measurements were stored continuously. In addition the full strain cycle count was stored on tape.

Although it generally performed well, the DAU suffered from a recurring computer disk problem which caused some loss of data.

3. DESCRIPTION OF HYDRODYNAMIC MODEL

3.1 PROGRAMS USED

The WSA global load model has been developed using the wave loading programs in WSA's finite-element program suite ASAS (Atkins Stress Analysis System), developed in-house over the past 30 years, and very widely used by many organisations world-wide. The initial model was developed to compare results with a SESAM wave loading model used by Shell. Following a satisfactory comparison the model was modified to reflect the 'PRESENT-STATE' of the Tern platform and be representative of the loads contributing to the measured global load. The final ASAS model is illustrated in Figure 3.1.

3.2 MODELLING PHILOSOPHY

In general, the philosophy throughout the modelling was to follow current practice in the UK offshore industry, at every stage.

The main jacket structure was modelled using TUBE elements. In general each element was defined between intersecting centre lines with no work point offsets and was of constant section size along its entire length. Exceptions were as follows:

- Segmented members were used where changes in diameter occur (i.e. where members go through the splash zone or at major changes in leg section);

- Segmented members were used where significant changes in diameter occur due to node cans;

- Where cone members are indicated the average diameter were taken;

- Brace offsets to the face of leg members were modelled.

The following specific modelling points should be noted:

- Where changes in member diameter are called for along the length of a member the wave loading effects of the changes are automatically included;

- Work point offsets in excess of 25% of chord diameter have not been included, as normally required for a stiffness analysis, as these will have a minimal effect on wave loading;

- Only main leg members and open ended caissons have the potential to be flooded and therefore only these members need true representations of member thickness to correctly model buoyancy effects. Other members were allocated a nominal thickness.

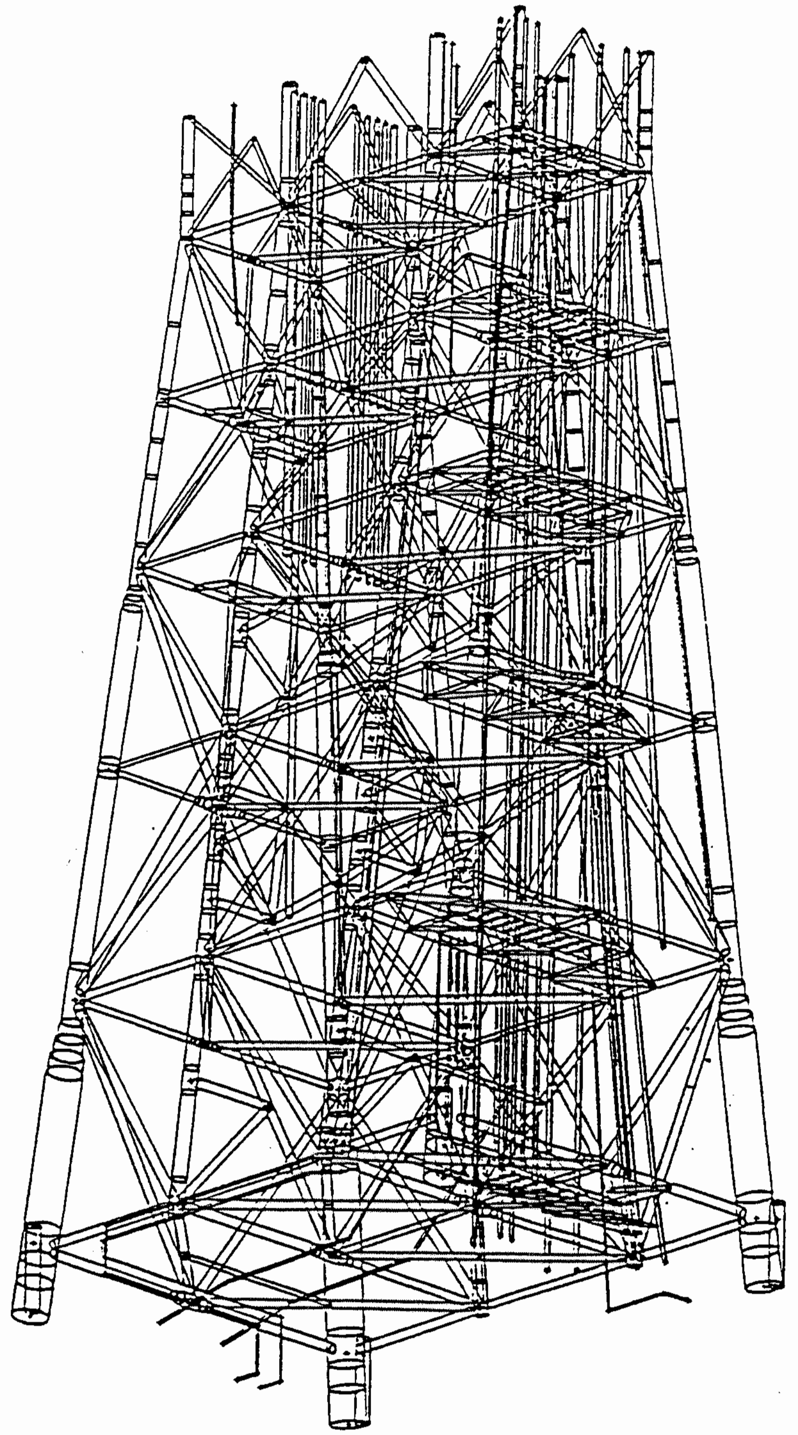

TERN JACKET - ISOMETRIC VIEW

Figure 3.1
ASAS model of Tern jacket

There were several areas which required additional modelling attention as follows:

- Conductor ladder members were modelled as single members with appropriate values of C_D and C_M;
- Pile sleeve assemblies were modelled by a single member simulating each pile sleeve assembly;
- Top of jacket plan bracing level reflected the loading effects of the top of jacket walkway;
- Jacket legs included ladders to sea level;
- Launch legs A2 and A3 included the launch box and launch runners.

3.3 ASSUMPTIONS MADE

The assumptions made throughout the hydrodynamic modelling followed current practice in the offshore industry.

3.3.1 Appurtenances

Appurtenances included risers, caissons, J-tubes and conductors. The wave loading caisson was assumed to be permanently developed.

3.3.2 Deck Modelling

The deck is not modelled. However, deck legs were modelled to the underside of the deck to ensure that all members exposed to wave loading were included in the analysis.

3.3.3 Shielding

No account was taken of the effects of shielding. Only some of the conductors were installed on Tern at the time of the experiment, so this is a reasonable assumption.

3.3.4 Marine Growth

A marine growth allowance of 50mm was added to all members and appurtenances between +2.3m and -40m with respect to nominal LAT.

3.3.5 Current

The effect of current on the peak-to-peak wave loads considered in this experiment is small. This is because the current magnifies the load peaks of one sign, but almost equally reduces the load peaks of the other sign, leaving the peak-to-peak load almost unchanged. Accordingly, all the results in the main part of this Report are based on ASAS runs with the current velocity set to zero, for simplicity.

However, in all but three of the 1-hour records considered, current data was available, see Table 4.1. Therefore, the ASAS runs were repeated in these cases, with the current included. The results are given in Appendix 2, for completeness. It may be seen that the resulting values of the conservatism parameters are reduced, on average, by about 2%. These changes are not statistically significant, at any rate when considered individually, see Section 5.

3.3.6 Tide/Storm Surge: Mean Water Levels

The model had provision to vary the mean water level to suit the tide and storm surge. This data was available experimentally as the 1-hour mean water level (MWL), see Table 4.1. This figure was generally used for the mean water level in the computer wave kinematics model below. Since this meant that the crest elevation of the model wave did not match that of the actual wave (although its height did, see 3.3.7 below), some additional runs were performed with the mean water level adjusted so that (in addition) the crest elevation matched the measurements. These were in the most severe 1-hour record, i.e. record 12 in Table 4.1 of Section 4 below. See Appendix D of RPT/009 of the WSA Final Report[3].

The 25 large waves in this record yielded individual values of R_{cycle} which occasionally differed from those obtained previously (i.e. without the mean water level adjustment). However, the mean of these 25 values was 0.80 for BSF, and 0.83 for OTM, with standard deviations of 0.17 and 0.22 respectively. This is a negligible change from the overall results for that record obtained previously, see Table 5.1. As for the largest individual wave in the record (illustrated in Figure 5.1), which was also responsible for the largest wave load, the values of R_{cycle} were 0.90 for both BSF and OTM, which was no change on the figures obtained previously.

3.3.7 Wave Kinematics

Following conventional practice, a Stokes 5th order regular wave model was adopted throughout. For each run in Section 5, the direction was set to the experimentally-measured figure given in Table 4.1. The great majority of the runs were then performed with the wave height and period set to the measured height (crest to following trough) and period (between upcrossings) of individual waves. The remaining runs (to find R_{stat}) were performed with theoretically-determined wave height and period, see Section 5.

3.3.8 Wave Load Coefficients

The transverse wave load per unit length of structural member is defined by Morison's equation, viz:

$$\tfrac{1}{2}\rho C_D D V|V| + \rho C_M A\, dV/dt$$

Here D and A are the member diameter and cross-sectional area, ρ and V are the water density and transverse velocity, and C_D and C_M are the Morison drag and inertia coefficients.

Following standard UK practice[5] the transverse water acceleration dV/dt is taken to mean the transverse component of total particle acceleration. This means that it includes the convective acceleration term (i.e. $(\nabla V)V$ in tensor notation) which is responsible for the fluid acceleration in steady flow (e.g. in a narrowing pipe), as well as the more obvious unsteady-flow term equal to the rate-of-change of velocity $\partial V/\partial t$ at a fixed point. In other words:

$$dV/dt = \partial V/\partial t + (\nabla V)V$$

Also following standard UK practice[5] axial inertial forces (axial Froude-Krylov forces) are included too, by means of an effective inertia coefficient of 1.00 in that direction. These are the simplest of the mathematical refinements, recently comprehensively derived[12], which are possible to the original Morison inertia term.

The Morison coefficients have been taken at the standard values, as follows:

Drag Coefficient (C_D)	=	0.70
Mass Coefficient (C_M)	=	2.00

Where anodes were fitted to the structure, which is on most members except the conductors, the drag coefficient of 0.70 was increased by 6%, which is appropriate in view of their contribution to drag forces.

The following areas are not considered for wave loading purposes:

- M&E pipework (i.e. the small-bore "mechanical and electrical" pipework, which is in practice mainly the air-vent pipes for the flooding systems);

- Appurtenance supports.

3.3.9 Buoyancy Loads

The primary effect of buoyancy is a static vertical force. Dynamic changes in buoyancy occur with the passage of the wave due to changes in local water surface elevation across the structure. This effect is automatically included by ASAS in the calculation of overturning moment.

3.3.10 Wind Loads

As wind loads are very low frequency in nature they were not included in the analysis.

3.3.11 Jacket Dead-weight and Topside Loading

As dead-weight and topside loading effects are static in nature they were not included in the analysis.

4. DATA COLLATION AND PROCESSING

A total of 15 storms were selected for detailed analysis; these included all storms when the significant wave height was above 8m for which good quality data was obtained.

All global load time history data have been subject to a low pass filter at $0.3H_z$ (in addition to SM's basic 2 Hz anti-aliasing filter) to remove dynamic effects due to platform structural response to wave loading. Since the Tern load data is essentially oscillatory, as noted in Section 2.1, range values, (i.e. peak-to-following-trough values with the first peak corresponding to a wave crest) are used throughout. The period associated with a given cycle is the time between the zero-crossing before the first peak, and that after the trough. In addition the following statistical parameters were obtained:

- Standard deviation for waves, 4 x standard deviation = significant wave height;
- Maximum range value found in record;
- Mean zero crossing period (of waves);
- Peak spectral period
- Directional spreading (of waves);

Tables 4.1 and 4.2 show these parameters as measured over the worst-case 1-hour record in each of the 15 selected storms. For the two severest storms (17/18 October 1991 and 1 January 1992) a succession of eight 1-hour records are also considered, around the worst-case record. The key wave data is shown pictorially in Figure 4.1

The highest wave of 26.92m was recorded on 1 January 1992, in the one-hour record beginning at 06:00 hours. The maximum global load ranges in this record were a base shear force (BSF) of 62.4 MN and an overturning moment (OTM) of 9,337 MNm, see Table 4.2, both occurring in the highest wave. Table 4.2 shows SM's final figures for BSF and OTM, incidentally - the WSA analysis used earlier, less refined, versions where the extremes of both BSF and OTM were on average 1.0% higher.

SM undertook consistency checks on all the processed data with a significant wave height exceeding 8m. Three types of analysis were undertaken on selected recordings:

- General plotting and overall studies
- Deterministic individual cycle analysis
- Spectral and probabilistic analysis

In general WSA has utilised the results from the first two analyses only.

Table 4.1
Details of Selected Storm Records

Rec. No.	Storm Date	Record Start (GMT)	H_S (m)	H_{max} (m)	T_Z (secs)	T_P (secs)	Wave Dirn (degs)	MWL (m)	V_x (m/s)	V_y (m/s)	Max s	Avrg φ
1	20/2/90	3	9.81	14.55	9.77	13.0	283	na	na	na	20	0.65
2	20/9/90	5	8.36	14.38	9.85	15.0	331	na	na	na	8	0.71
3	16/4/91	13	9.00	15.16	10.39	14.0	377	-0.17	0.03	-0.03	15	0.73
4	22/5/91	0	9.40	15.87	9.73	13.0	298	0.02	na	na	na	na
	17/10/91	22	11.6	18.9	11.3	15.0	21	-0.20	0.09	-0.49	7	0.70
	17/10/91	23	11.6	21.1	10.7	15.0	21	-0.40	0.10	-0.41	7	0.70
	18/10/91	0	11.5	16.9	11.0	15.0	26	-0.50	0.10	-0.41	7	0.69
	18/10/91	1	11.3	17.8	10.2	16.0	31	-0.50	0.09	-0.37	9	0.69
5	**18/10/91**	**2**	**12.11**	**20.48**	**11.04**	**15.0**	**29**	**-0.40**	**0.08**	**-0.35**	**10**	**0.71**
	18/10/91	3	11.0	22.8	10.3	16.0	31	-0.30	0.08	-0.33	8	0.68
	18/10/91	4	11.4	20.2	10.6	15.0	32	0.00	0.08	-0.34	6	0.60
	18/10/91	6	10.5	17.8	10.1	16.5	33	-0.20	0.07	-0.34	7	0.67
6	1/11/91	3	9.38	14.95	8.98	13.0	162	-0.20	0.01	0.02	10	0.75
7	4/11/91	20	7.96	12.96	9.38	14.0	36	0.60	0.06	-0.27	12	0.75
8	11/11/91	13	8.18	15.52	9.28	16.0	290	0.90	-0.02	0.01	30	0.70
9	18/12/91	7	9.34	14.08	10.20	18.0	295	0.70	-0.05	-0.06	30	0.76
10	19/12/91	17	10.20	14.96	9.76	15.0	275	0.80	-0.03	0.02	8	0.69
11	22/12/91	22	10.36	15.16	9.42	14.0	295	1.00	-0.25	0.10	8	0.67
	1/1/92	1	7.8	13.5	8.4	11.0	228	0.01	0.06	0.06	3	0.56
	1/1/92	2	8.9	16.6	8.7	13.0	233	0.18	0.08	0.17	3	0.59
	1/1/92	3	10.8	23.9	9.0	14.0	262	0.55	0.00	0.27	3	0.46
12	**1/1/92**	**6**	**13.78**	**26.92**	**11.08**	**15.0**	**281**	**0.65**	**-0.25**	**0.27**	**18**	**0.72**
	1/1/92	7	12.5	19.7	10.6	15.0	287	0.64	-0.34	0.23	15	0.68
	1/1/92	8	11.3	17.9	9.9	15.0	286	0.47	-0.31	0.13	12	0.62
	1/1/92	11	9.5	15.1	9.9	12.5	289	-0.08	-0.02	0.01	8	0.60
	1/1/92	12	8.6	14.5	9.3	13.0	291	-0.16	-0.02	0.02	6	0.55
13	22/2/92	5	8.35	13.07	8.76	11.0	269	-0.41	-0.02	0.14	9	0.62
14	14/3/92	21	8.14	15.92	9.09	12.5	6	0.17	-0.02	-0.09	11	0.70
15	18/4/92	17	9.10	16.75	9.38	13.0	293	-0.65	0.06	0.01	22	0.76

T_P - *Period Corresponding to peak of wave spectrum.*

Dirn - *Mean direction waves are coming from relative to platform N, as deduced from V_x, V_y*

V_x, V_y - *Mean particle velocities at -41m, x = platform N, y = platform E.*

MWL - *Mean water surface elevation relative to MSL (+ve up); MSL = nominal LAT + 1.05m.*

Max s - *Value of spreading function s at peak of wave spectrum, $s = \varphi/(1-\varphi)$*

Avrg φ - *Average value of spreading function φ over range 0.05 to 0.15 Hz*
If Sxx, Syy, Sxy are spectra and cross-spectra of V_x, V_y then

$$\varphi = \frac{(4S^2xy + (Sxx - Syy)^2)^{1/2}}{Sxx + Syy}$$

This is strictly-speaking the 2nd angular harmonic of the directional part of the wave spectrum, see Tucker[13] eqns 7.3-30, 7.3-31. If waves are unidirectional $\varphi = 1$.

Table 4.2
Details of Selected Response Records

Record No	Storm Date	Record Start (GMT)	BSF max (MN)	BSF sd (MN)	OTM max (MNm)	OTM sd (MNm)	pv41 max (m/s)	pv41 s.d. (m/s)	BSF/ wv.ht. MN/m	Correl- ation
1	20/2/90	3	28.3	3.17	4047	418	2.40	0.36	1.0	0.57
2	20/9/90	5	24.0	2.91	3255	375	1.62	0.24	1.2	0.77
3	16/4/91	13	22.4	3.02	3060	390	2.16	0.31	1.5	0.78
4	22/5/91	0	25.9	3.49	3528	464	na	na	1.3	0.69
	17/10/91	22	31.0	4.67	4269	616	2.59	0.40	1.7	0.78
	17/10/91	23	32.2	4.62	4464	613	2.47	0.39	1.6	0.75
	18/10/91	0	37.6	4.78	5361	628	2.59	0.42	1.8	0.73
	18/10/91	1	36.1	4.50	5166	590	3.06	0.39	1.9	0.78
5	**18/10/91**	**2**	**38.0**	**4.84**	**5439**	**635**	**3.14**	**0.42**	**1.7**	**0.74**
	18/10/91	3	36.5	4.41	4971	580	3.06	0.40	1.8	0.83
	18/10/91	4	33.3	4.42	4260	588	2.55	0.40	1.8	0.75
	18/10/91	6	32.9	3.79	4659	498	2.55	0.35	1.4	0.70
6	1/11/91	3	25.9	2.90	3723	384	1.79	0.27	1.3	0.77
7	4/11/91	20	19.7	2.56	2710	339	1.58	0.25	1.4	0.84
8	11/11/91	13	20.9	2.71	2827	351	2.20	0.28	1.3	0.69
9	18/12/91	7	25.2	3.36	3099	413	2.05	0.34	1.6	0.75
10	19/12/91	17	24.8	3.55	3606	472	2.13	0.33	1.3	0.61
11	22/12/91	22	30.6	3.65	4503	501	2.13	0.35	1.5	0.69
	1/1/92	1	14.6	1.83	2164	263	1.31	0.18	0.7	0.57
	1/1/92	2	21.3	2.55	3177	369	1.66	0.24	1.1	0.69
	1/1/92	3	31.8	3.23	4971	476	2.09	0.28	1.0	0.58
12	**1/1/92**	**6**	**62.4**	**5.36**	**9337**	**714**	**4.58**	**0.48**	**1.8**	**0.76**
	1/1/92	7	32.2	4.62	4659	611	2.83	0.43	1.4	0.70
	1/1/92	8	31.8	3.79	4425	495	2.55	0.39	1.0	0.53
	1/1/92	11	24.0	2.88	3450	373	2.05	0.32	1.1	0.68
	1/1/92	12	19.7	2.56	2593	329	1.85	0.30	0.6	0.45
13	22/2/92	5	17.7	2.10	2827	282	1.54	0.23	0.8	0.56
14	14/3/92	21	19.3	2.39	2632	307	1.42	0.23	1.2	0.72
15	18/4/92	17	25.9	3.12	3762	412	1.93	0.29	1.2	0.74

Directions - *BSF,OTM and pv41(i.e. PVM at 41m) data all have means removed, and are then resolved in mean wave direction shown in Table 4.1*

Max - *measured max range. Note that this is different from the ranges used in the definition of the conservatism parameters, which are the ranges of:*

$$\{(\text{northerly load})^2 + (\text{easterly load})^2\}^{1/2}$$

s.d. - *standard deviation*

BSF/wv.ht. - *ratio obtained by best line fit to individual cycle data*

Correlation - *correlation coefficient of BSF and waveheight, individual cycle data*

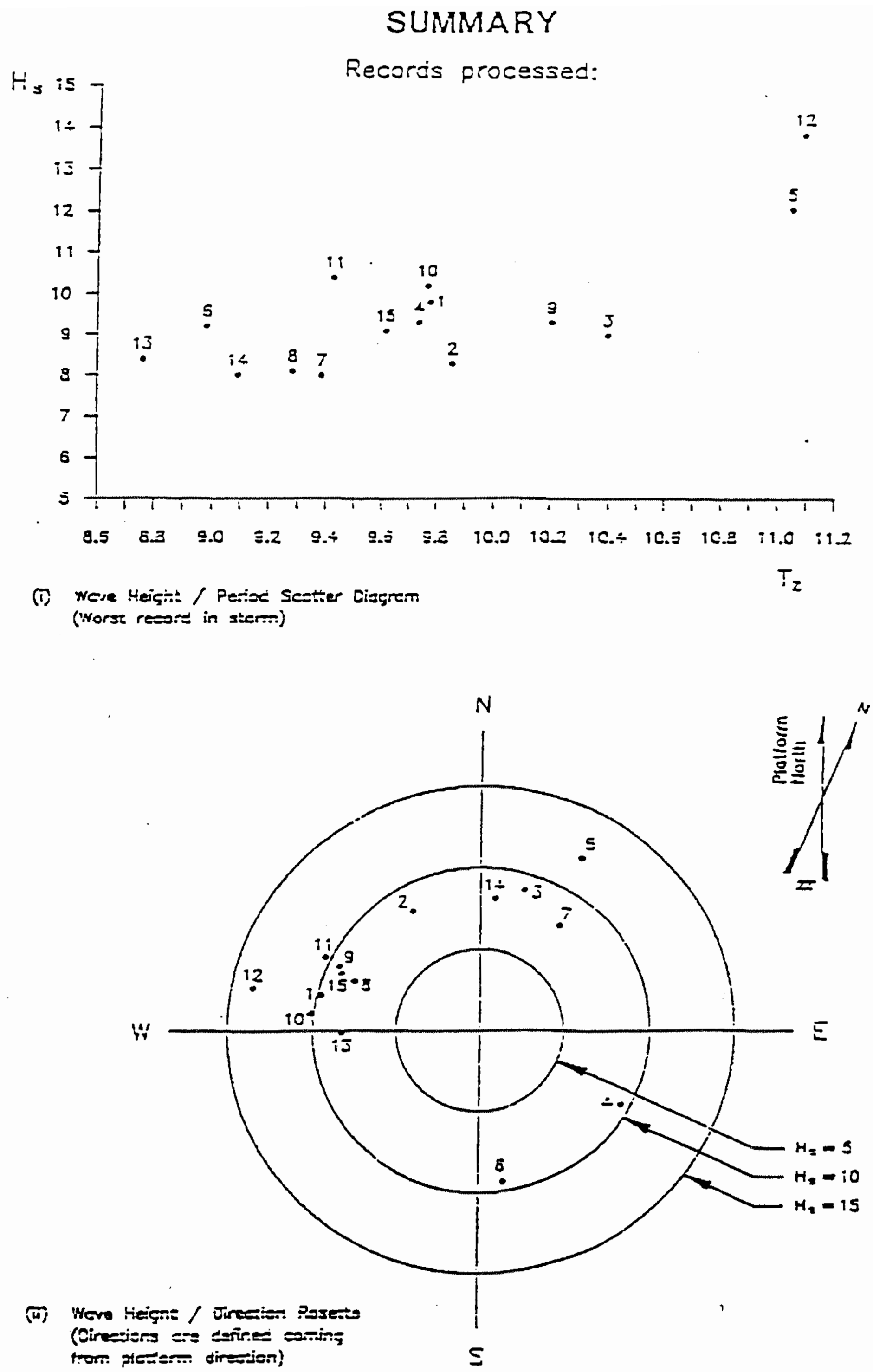

Figure 4.1
Key Parameters of Selected Storms

5. RESULTS

5.1 AVERAGE CONSERVATISM, OVER ALL LARGE WAVES

The 25 largest waves in each of the 15 1-hour records identified in Table 4.1 (i.e. 375 waves in all) were individually modelled as described in Sections 3.3.6 and 3.3.7., and the peak-to-peak shear force and overturning moment was computed. This was compared with the peak-to-peak shear force and overturning moment, as defined in Section 4. The conservatism in the calculation was then defined by the ratio:

$$R_{cycle} = \frac{\text{measured peak-to-peak wave load in single wave}}{\text{computed peak-to-peak wave load in same wave}}$$

which was obtained for both base shear force (BSF) and overturning moment (OTM). For each 1-hour record, Table 5.1 below shows the average and standard deviation (s.d.) of the 25 values of R_{cycle} obtained in this way, in that record.

Table 5.1
Average values of individual-wave conservatism parameter R_{cycle}

Record No	Measured Significant Wave Height (m)	Measured Zero Cross Period (s)	R_{cycle} for BSF average	R_{cycle} for BSF s.d.	R_{cycle} for OTM average	R_{cycle} for OTM s.d.
12	13.78	11.08	0.80	0.17	0.84	0.21
5	12.11	11.04	0.85	0.22	0.93	0.26
11	10.36	9.42	0.82	0.25	0.87	0.29
10	10.20	9.76	0.77	0.26	0.79	0.29
1	9.81	9.77	0.70	0.21	0.73	0.27
4	9.40	9.73	0.81	0.22	0.83	0.26
6	9.38	8.98	0.83	0.18	0.85	0.19
9	9.34	10.20	0.73	0.17	0.79	0.22
15	9.10	9.81	0.78	0.19	0.82	0.24
3	9.00	10.39	0.80	0.19	0.83	0.20
2	8.36	9.85	0.79	0.17	0.79	0.18
13	8.35	8.76	0.64	0.12	0.64	0.13
8	8.18	9.28	0.72	0.19	0.74	0.22
14	8.14	9.09	0.78	0.17	0.78	0.19
7	7.96	9.38	0.79	0.15	0.79	0.14
Overall Average (= Av[averages])			0.77		0.80	
Overall s.d.(= $\{Av[(s.d.)^2]+(s.d.[avs])^2\}^{1/2}$)				0.20		0.23

It can be seen that the average values of R_{cycle} are substantially less than 1.0, implying that the load calculation is, on average, conservative. Given the number of data points (15×25 = 375), the standard[9] statistical test (the Student t-distribution) gives the 95% confidence limits for the true average values of R_{cycle} as $\pm 1.65/\sqrt{375} = 0.085$ standard deviations, which is $\pm 0.085 \times 0.20 = \pm 0.017$ and $\pm 0.085 \times 0.23 = \pm 0.020$ respectively. The conservatism is thus statistically highly significant, and is the first important finding in the WSA Final Report[3]. The result has been confirmed by other analyses[4] of the Tern data, and shown to be consistent with the results of earlier experiments on the Magnus platform, and the Ocean Test Structure in the Gulf of Mexico.

5.2 CONSERVATISM IN 1-HOUR EXTREME LOADS

The Tern experiment also investigated the conservatism in the prediction of 1-hour the extreme load in a 1-hour record. This was measured firstly by:

$$R_{det} = \frac{\text{largest of the 25 measured loads in a 1-hour record}}{\text{largest of the 25 computed loads in a 1-hour record}}$$

Note that, unlike R_{cycle}, the measurement and computation *need not come from the same wave*. The other whole-record parameter was based on the largest wave in that record, as predicted by standard statistical methods, from the measured wave spectrum. The load in this theoretical wave was computed, to give:

$$R_{stat} = \frac{\text{largest of 25 measured loads in 1-hour record}}{\text{load computed in theoretical largest wave for that record}}$$

Table 5.2 below shows the values of R_{det} and R_{stat} , from the 15 1-hour storms records:

Table 5.2
Whole-record conservatism parameters R_{det} and R_{stat}

Record No	Measured Maximum Wave Height	Predicted Maximum Wave Height	R_{det} BSF	R_{det} OTM	R_{stat} BSF	R_{stat} OTM
12	26.92	23.44	0.90	0.90	1.16	1.14
5	20.48	20.60	0.85	0.96	0.86	0.98
11	15.16	17.87	1.16	1.32	0.90	0.93
10	14.96	17.53	0.96	1.00	0.73	0.70
1	14.55	16.87	1.07	1.37	0.91	0.87
4	15.87	16.16	0.95	0.94	0.89	0.91
6	14.95	16.25	1.10	1.19	0.95	1.05
9	14.08	15.99	1.01	1.00	0.85	0.76
15	16.75	15.64	0.90	0.95	0.91	1.02
3	15.16	15.38	0.89	0.90	0.78	0.88
2	14.38	14.36	1.02	1.06	0.96	1.06
13	13.07	14.48	0.92	0.98	0.78	0.85
8	15.52	14.12	0.76	0.75	0.85	0.87
14	15.92	14.07	0.84	0.77	0.83	0.87
7	12.96	13.72	1.04	0.99	0.83	0.88
Average			0.96	1.01	0.88	0.92
Std Dev			0.11	0.17	0.10	0.12

The whole-record conservatism revealed by the average values of R_{det} and R_{stat} appears to less than the individual-wave conservatism of the earlier Table 5.1. Given the number of data points (15), the standard statistical test used earlier gives the 95% confidence limits for the true average values of R_{det} and R_{stat} as $\pm 1.75/\sqrt{15} = 0.45$ standard deviations. For R_{det} this is $\pm 0.45 \times 0.11 = \pm 0.050$ for BSF and $\pm 0.45 \times 0.17 = \pm 0.077$ for OTM. For R_{stat} it is $\pm 0.45 \times 0.10 = \pm 0.045$ and $\pm 0.45 \times 0.12 = \pm 0.054$ respectively. The difference between whole-record and individual-wave conservatism is thus statistically highly significant. This is the second important finding in the WSA Final Report(3).

There is also an important additional point, concerning R_{stat} . It arises because the "standard statistical methods" used to predict the theoretical maximum wave height[1] in each record (and hence define R_{stat} , see above) were the simplest available, and used the asymptotic Rayleigh formula:

$$H \quad = \quad H_S \times \sqrt{[0.5 \times \log_e(3600/T_Z)]}$$

to give the 1-hour maximum waveheight H from the measured significant waveheight H_S and zero-crossing period T_Z. In wave forecasting, however, this simple formula is first corrected for finite record duration. In the present case of 1-hour (about 360 wave) record lengths, this requires a multiplier (mathematically derived(10) from the Rayleigh distribution) of(6) 1.038, in order to give a value of H which is unbiased (i.e. correct on average, as required for present purposes, in which averaged data is considered). Then, an additional multiplier is included, to allow for the finite width of the spectrum, and the non-linearity of the waves. In UK waters, the value of this latter multiplier is taken(7) as 0.9, based an analysis(7),(8) of storms around the UK.

Thus overall, wave forecasters would expect their extreme wave heights, in present case of 1-hour records taken in UK waters, to have an average value of $1.038 \times 0.9H = 0.93H$. If this is incorporated in the above definition of R_{stat} , it will reduce the computed wave load by a factor of between 0.93 and $(0.93)^2$, depending whether the wave loading is dominated by inertia or drag forces. This will increase the resulting value of R_{stat} by approximately 10%, in the present case where drag forces are important, but not always dominant.

5.1 WAVE KINEMATICS

The overall accuracy of conventional wave loading calculations, shown in Table 5.2, may of course be fortuitous. The conventional calculation may first over-estimate the water velocities (i.e. the wave kinematics), and then under-estimate the wave load produced by these velocities. Or vice-versa. Whether this is the case may be seen by examining the measured water velocities. That data is only given in the WSA Final Report(3) for one wave, which was the largest and most-forceful one seen in the whole experiment, on 1 January 1992. This gives a limited, but pertinent, check on wave kinematics.

The data is shown in Figures 5.1 and 5.2. First, Figure 5.1 shows the surface profiles as measured by the two wave gauges (see Figure 2.1), plotted on the same vertical scale (m above nominal LAT). Only the EMI sensor data was made use of, see Section 2.1.1. The Marex data is included here because of the inherent interest of the wave, in view of its

---

[1] the wave period associated with this theoretical maximum height was taken as the least favourable value from the range $1.05T_Z$ to $1.41T_Z$, following standard UK practice(5). The load variation over this range is only important in relatively small N/S waves - here the platform spans a significant portion of a wavelength, so longer periods produce significantly bigger loads. This produced very little extra conservatism in R_{stat} , however, since the waves responsible for the extreme wave loads had their periods at the upper end of the range anyway, and sometimes beyond it.

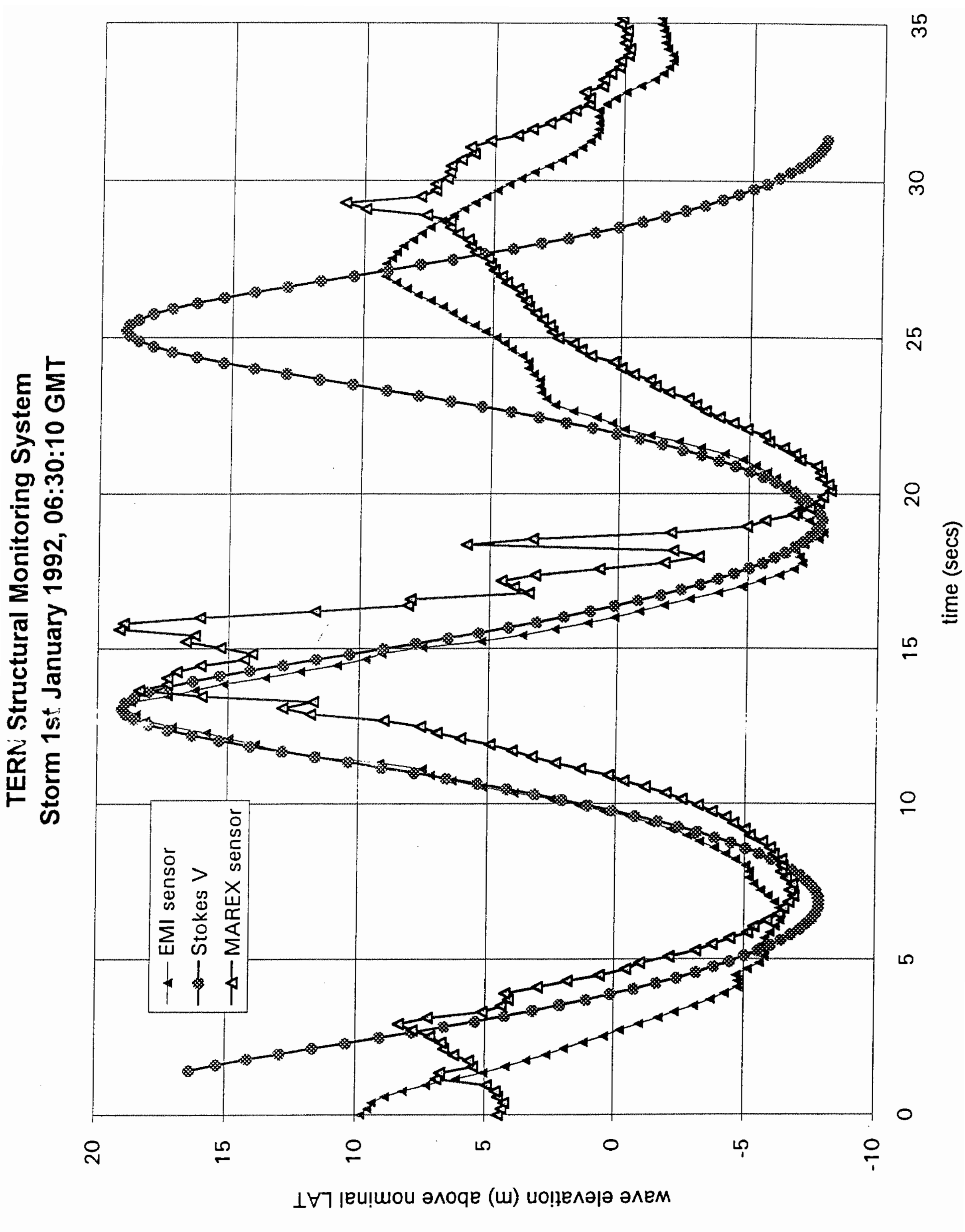

Figure 5.1
Surface profile of largest wave seen during experiment

steepness (its height of 26.92m and zero-crossing period of 12.50 seconds give it a nominal length/height ratio of 9.06:1, which is outside conventional guidelines[2]). Superimposed is the wave profile (at the position of the EMI sensor) used in conventional wave loading calculations - this is a Stokes 5th order regular wave, fitted to the measured wave height and zero-crossing period, as described in Section 3.3.7. As an additional refinement, its mean level is adjusted (by 1.49m upwards from hourly MWL in this case) as described in Section 3.3.6, so that its crest elevation, as well as its height, matches the data. This gives the most pertinent comparison with the velocity measurements, since the issue is of course the accuracy of the whole velocity field used in the wave load calculation. If the mean level is not adjusted in this way, the velocity will appear to be slightly overpredicted (by about $e^{1.49\times0.02576} = 3.9\%$, in fact, see below) when in reality the whole velocity field has merely been shifted vertically, with negligible effect on the loading, see Section 3.3.6.

Figure 5.2 shows the corresponding data from the water velocity sensor (oscillatory velocity only, resolved in the mean wave direction, see note in Table 4.2), located 41m below nominal LAT, and offset from the wave sensors, as described in Section 2.1.1. Superimposed is the velocity from the Stokes wave of Figure 5.1, at the same location. This is of course a very standard calculation for the ASAS software, but can nevertheless be cross-checked, by comparison with another program, written by J.R.Chaplin using a stream-function solution[14]. According to the Chaplin program, a wave of the same height, period, and mean level gives peak velocities at the sensor of +2.171 m/s and -2.118 m/s, in very close agreement with the ASAS Stokes prediction. It can also be cross-checked by comparison with a linear (Airy) wave of the same height, period, and mean level. In the present conditions, and with $g = 9.81$ m/s^2, the Airy wave number is 0.02576 m^{-1} (which is in fact the same as its value in deep water, to 4 significant figures). The mean level in the Stokes wave is 1.49m above hourly MWL (see above), and MWL in the present storm is 1.05+0.65 m above nominal LAT (see Table 4.1), so the velocity sensor is $41+1.49+1.05+0.65 = 44.19$m below the mean water level in the Stokes wave, and the seabed is $167+1.49+1.05+0.65 = 170.19$m below that level. Thus the velocity at the sensor in an Airy wave comes to:

$$\pm(26.92/2)(2\pi/12.50)\cosh[0.02576\times(170.19-44.19)]/\sinh(0.02576\times170.19) = \pm2.171 \text{ m/s}$$

which is also in close agreement with the ASAS Stokes prediction.

Having thus established that, as expected, there are no errors in the conventional kinematics calculation shown in Figure 5.2, the computed and measured velocity time-histories can be compared. After allowing for the phase difference, which is caused by the measurement delay-time of the Interocean PVM used (viz. about 2 seconds), it may be seen that the peak-to-peak values (used throughout the experiment as the basis for comparison, see Section 4) are remarkably close.

Thus the one wave whose kinematics were presented in the WSA Final Report[3], which was the largest and most-forceful (and therefore the most important) wave seen in the whole experiment, is entirely supportive of the use of Stokes wave kinematics.

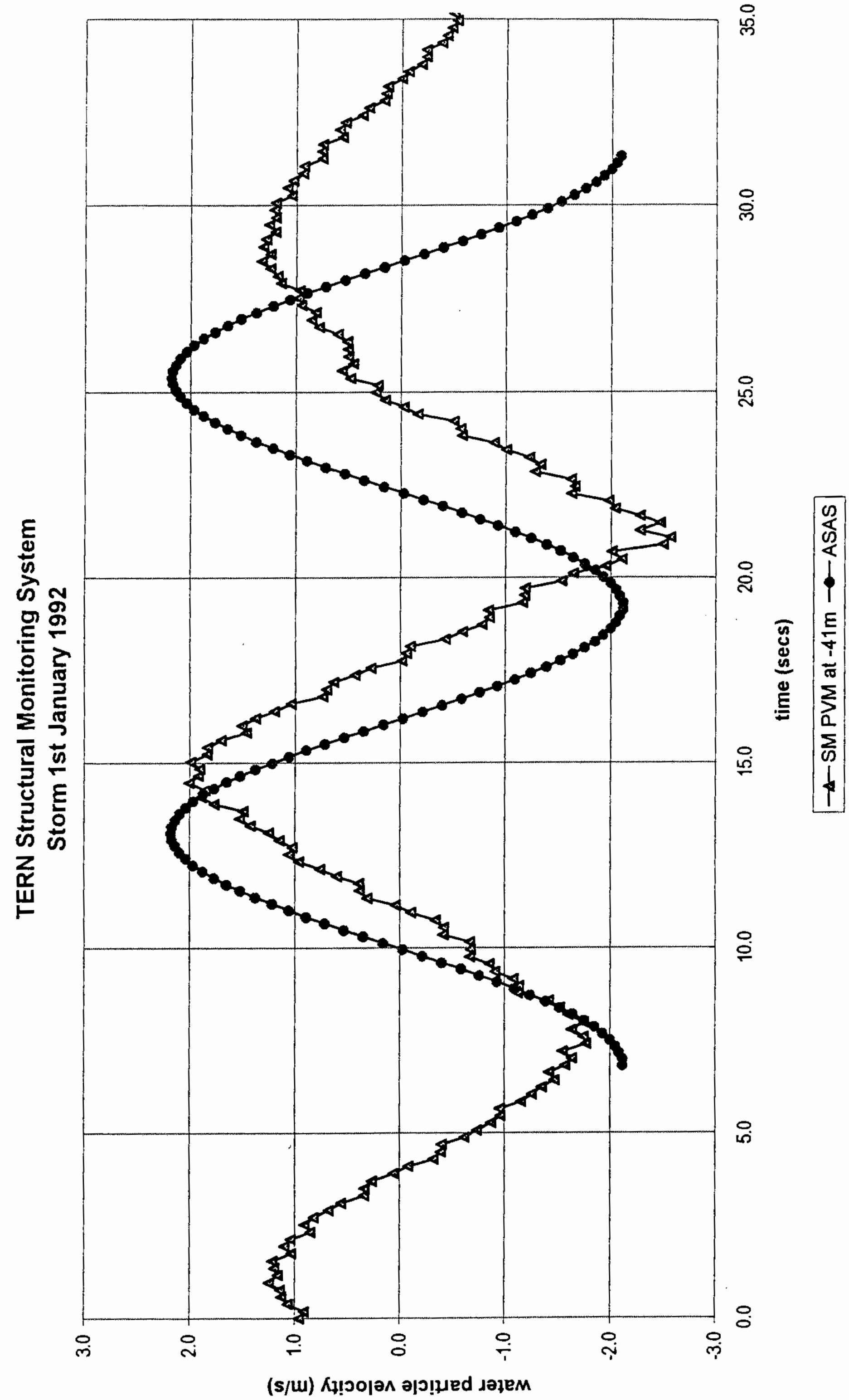

Figure 5.2
Velocity profile of largest wave seen during experiment

6. CONCLUSION

The Tern wave load measurement programme is perhaps the most important experiment of this type performed anywhere in the world, up to the present time.

The environmental and structural sensors both behaved in an exemplary fashion, and continued to do so over a number of winter seasons, during which there were several exceptionally severe storms. As a result, very high quality data was obtained.

This Report summarises its analysis by WS Atkins, as a Joint Industry Project aimed at verifying, or otherwise, current UK design practice.

The conclusion is that current UK design practice appears to be very realistic, with little or no overall conservatism in its predictions of extreme wave loads. However, the experiment did not address the important issue of combining extreme current and wave loads, in a rational manner. This was inherently beyond the scope of the experiment, because only oscillatory loads were measured.

REFERENCES

1. BEA, R., LOCH, K., & YOUNG, P.
Evaluation of storm loading imposed on and induced in template-type offshore platforms in their ultimate limit state
5th ISOPE (Intl. Soc. Offshore & Polar Engrs) Conference, The Hague, 1995

2. AMERICAN PETROLEUM INSTITUTE
Recommend Practice for Planning, Designing, and Constructing Fixed Offshore Platforms
API Recommended Practice RP2A, 20th Edition, July 1993

3. ATKINS OIL & GAS ENGINEERING LTD.
Tern Structural Loading Study: Final Report
Atkins Oil & Gas Engineering Report, Ref. G3356/RPT, May 1993

4. HEIDEMAN, J.C. & WEAVER, T.O.
Static wave force procedure for platform design.
Proc. 5th Int. Conf. on Civil Engineering in the Oceans, College Station, Texas. ASCE, November 1992

5. UK HEALTH & SAFETY EXECUTIVE
Offshore Installations: Guidance on design, construction and certification. 4th Ed.
London: HMSO, 1990

6. FORRISTALL, G.Z.
On the statistical distribution of wave heights in a storm
J.Geophys.Res. Vol 83 No C5, 2353-2358, 1978

7. UK DEPARTMENT OF ENERGY
Metocean Parameters - Wave Parameters. Supporting document to "Offshore Installations: Guidance on Design, Construction & Certification - Environmental Considerations"
Offshore Technology Report OTH 89 300. London: HMSO, 1989

8. HOGBEN, N. & CARTER, D.J.T.
Estimation of extreme wave heights: a review of guidance issued by the UK Department of Energy.
Underwater Technology, vol 18 no.1., 1992.

9. KREYSIG, E.
Advanced Engineering Mathematics, 4th Ed.
New York: John Wiley & Sons, 1979

10. LONGUET-HIGGINS, M.S.
On the statistical distribution of the heights of sea waves
J. Mar. Res. Vol 11(3), 245-266, 1952

11. JOHNATHAN, P. & TAYLOR, P.H.
Irregular nonlinear waves in a spread sea
14th OMAE (Offshore Mechanics & Arctic Eng.) Conference, Copenhagen, 1995

12. RAINEY, R.C.T.
Slender-body expressions for the wave loads on offshore structures
Proc. R. Soc. Lond. Vol A450, pp 391-416, 1995

13. TUCKER, M.J.
Waves in Ocean Engineering: Measurement, Analysis, Interpretation
New York: Ellis Horwood, 1991

14. CHAPLIN, J.R.
Developments of stream function wave theory
Coastal Engineering, Vol 3, pp 179-205, 1980

APPENDIX 1: COMPARISON OF BROADSIDE AND END-ON LOAD CASES

It has been noted in the literature[4] that the wave-by wave conservatism (i.e. amount that R_{cycle} falls short of 1.0) on Tern appears, on average, to be slightly more pronounced in waves hitting the platform broadside-on (i.e. waves travelling E-W or W-E) than it is in waves hitting the platform end-on (i.e. waves travelling N-S or S-N). This can be seen in Table 5.1, or, more precisely, in Table A2.1, where the effect of the current is included. On the other hand, this effect is *not* seen in the whole-record conservatism parameters R_{det} and R_{stat} , see Table 5.2, or, again more precisely, Table A2.2. These observations are summarised in Table A1.1 below, in which the 12 records of Tables A2.1 and A2.2 are divided into the N/S group (viz. the 5 records 3,5,6,7&14) where the waves approached within 45° of the platform N/S axis, and the E/W group (viz. the 7 other records) where they were within 45° of its E/W axis (see Figure 4.1).

Table A1.1
Differences between broadside and end-on waves

Parameter	R_{cycle}		R_{det}		R_{stat}	
	BSF	OTM	BSF	OTM	BSF	OTM
Overall average	0.755	0.783	0.938	0.973	0.857	0.903
Average over N/S waves	0.808	0.844	0.950	0.984	0.850	0.940
Average over E/W waves	0.717	0.739	0.929	0.966	0.861	0.876
% difference in N/S & E/W averages	12.7%	14.2%	2.3%	1.9%	-1.3%	7.3%
statistically-significant % difference	±6.5%	±7.3%	±13.9%	±17.0%	±12.4%	±14.7%

The Table gives the average values of R_{cycle} , R_{det} and R_{stat} over the two groups, and the percentage difference between them. Some difference is of course to be expected because of statistical scatter - in the last row, therefore, is the percentage difference which counts as statistically significant (at the 95% confidence level - i.e. there is only a 5% probability of such a difference, or greater, occurring by chance). This is readily calculated from the number of data points; in the case of R_{cycle} the two groups have 5×25 and 7×25 data points respectively, and in the case of R_{det} and R_{stat} they have 5 and 7 data points respectively. Thus the 95% confidence limits come to $\sqrt{(125^{-1} + 175^{-1})}$ and $\sqrt{(5^{-1} + 7^{-1})}$ times twice the standard deviations given in Tables A2.1 and A2.2.

It is immediately evident that for the case of R_{cycle} , the difference between broadside and end-on cases is statistically highly significant. One interpretation would be that this is an instrumentation problem - it could be argued that there is a difference in the strain gauge sensitivities for the two directions, of 13-14 %. However, this interpretation is not supported by the results for R_{det} and R_{stat} . If there were such a difference, the results there, taken together, are statistically significant evidence against it.

The most likely explanation appears to be that suggested by Shell[11], namely directional spreading of the waves. It can be seen from Figure 2.1 that waves from the West have their crests along the platform's long axis, whereas waves from the North or South have their crest along its short axis. Because of their short crests, therefore, directionally-spread seas achieve more spatial averaging, and thus on average lower wave loads, when from the East or West. This explains the difference seen in the average values of R_{cycle} above, because they are averages over all large waves in each record. In the case of R_{det} and R_{stat} , however, only the extreme load measurement is taken from each storm. This comes from an exceptionally forceful wave, which is likely to have little spreading, since spreading reduces wave load. An example of such a wave is given in Figures 5.1 and 5.2, where it is shown that the spreading appears to be negligible.

Thus it appears that the strain gauge sensitivities in the broadside and end-on directions are in fact the same, and thus both are probably correct.

APPENDIX 2: EFFECT OF CURRENT

Appendix H of RPT/009 in the WSA Final Report[3] gives the results of Section 5, re-computed with the current included, in all cases except records 1, 2 and 4 (where it was not available, see Table 4.1). These results are included here for completeness. Tables A2.1 and A2.2 below are direct replacements for Tables 5.1 and 5.2 in the main text, except that they have 12 records rather than 15, because of the three missing ones.

Table A2.1
Individual-wave parameter R_{cycle}, including effect of current

Record No	Measured Significant Wave Height	Measured Zero Cross Period (s)	R_{cycle} for BSF average	R_{cycle} for BSF s.d.	R_{cycle} for OTM average	R_{cycle} for OTM s.d.
12	13.78	11.08	0.75	0.16	0.78	0.19
5	12.11	11.04	0.85	0.22	0.95	0.26
11	10.36	9.42	0.64	0.12	0.64	0.13
10	10.20	9.76	0.77	0.26	0.79	0.29
6	9.38	8.98	0.83	0.18	0.85	0.19
9	9.34	10.20	0.73	0.17	0.79	0.22
15	9.10	9.81	0.77	0.26	0.79	0.29
3	9.00	10.39	0.80	0.19	0.83	0.20
13	8.35	8.76	0.64	0.12	0.64	0.13
8	8.18	9.28	0.72	0.19	0.74	0.22
14	8.14	9.09	0.78	0.17	0.78	0.19
7	7.96	9.38	0.78	0.15	0.81	0.14
Overall Average (= Av[averages])			0.76		0.78	
Overall s.d.(= $\{Av[(s.d.)^2]+(s.d.[avs])^2\}^{1/2}$)				0.20		0.23

Table A2.2
Whole-record parameters R_{det} and R_{stat}, including effect of current

Record No	Measured Maximum Wave Height	Predicted Maximum Wave Height	R_{det} BSF	R_{det} OTM	R_{stat} BSF	R_{stat} OTM
12	26.92	23.44	0.85	0.84	1.08	1.06
5	20.48	20.60	0.89	1.04	0.87	1.01
11	15.16	17.87	1.11	1.25	0.85	0.88
10	14.96	17.53	0.96	0.99	0.72	0.69
6	14.95	16.25	1.10	1.19	0.95	1.05
9	14.08	15.99	1.01	1.00	0.85	0.76
15	16.75	15.64	0.90	0.95	0.90	1.02
3	15.16	15.38	0.89	0.91	0.78	0.88
13	13.07	14.48	0.92	0.98	0.78	0.85
8	15.52	14.12	0.75	0.75	0.85	0.87
14	15.92	14.07	0.83	0.77	0.82	0.86
7	12.96	13.72	1.04	1.01	0.83	0.90
Average			0.94	0.97	0.86	0.90
Std Dev			0.11	0.14	0.09	0.11